

# NOLM and NALM based optical thresholders for interference suppression in optical code division multiplexing system

X. CHEN<sup>\*</sup>, Z. WANG, X. YUAN<sup>a</sup>

*College of Science, China Three Gorges University, Yichang, Hubei, P.R.China 443002, cxxg826@yahoo.com.cn*

*<sup>a</sup>Wuhan National Laboratory for Optoelectronics (WNLO), Huazhong University of Science and Technology, Wuhan, Hubei, P.R.China 430074*

Optical thresholders based on nonlinear optical loop mirror (NOLM) and nonlinear amplifying loop mirror (NALM) for interference suppression in optical code division multiplexing (OCDM) system are evaluated. The ratios of auto-correlation peak to the maximum wing level (P/W) and cross-correlation level (P/C) were used to quantitatively measure the interference suppression characteristic of the optical thresholders. The theoretical simulations show that system performance could be improve apparently by NOLM or NALM based on high nonlinear fiber (HNLF), and the results are validate by the corresponding experimental investigation in the 40 Gbit/s OCDM system.

(Received August 27, 2009; accepted September 30, 2009)

*Keywords:* optical thresholder, nonlinear optical loop mirror (NOLM), nonlinear amplifying loop mirror (NALM), high nonlinear fiber (HNLF), optical code division multiplexing (OCDM)

## 1. Introduction

Optical code division multiplexing (OCDM) is a promising technology for photonic packet switching or the optical LAN systems applications [1] due to its all-optical processing, flexible capacity, high information security, and so on. Recently, superstructured fiber Bragg grating (SSFBG) technology has emerged as an attractive and highly flexible route to produce high performance, and potentially low-cost choice for encoding/decoding in coherent phase-coding OCDM system [2].

Unfortunately, in the coherent OCDM system, there are three kinds of noise should be taken into account: multiple access interference (MAI), beat noise at the detector and receiver noise, and a key issue within the OCDM system relates to how to effectively suppress these noise. One can incorporate additional nonlinear components within SSFBG-based phase-coding scheme to improve the performance or to extend the functionality of this technical approach. Therefore, applying optical thresholding technique is crucial to achieve a practical OCDM system.

In the note, nonlinear optical loop mirror (NOLM) [3,4] based optical thresholder and nonlinear amplifying loop mirror (NALM) [5,6] based optical thresholder are analyzed and simulated, respectively. Theoretical investigation is compared with corresponding experimental demonstration in the 40 Gbit/s SSFBG-based OCDM system. The results show that system performance could be improved apparently by the

optical thresholding techniques based on the NOLM and the NALM.

## 2. System model of OCDM system

The system model of OCDM system is shown in Fig.1. A modelocked laser diode (MLLD) generates pulse train, after being modulated by electro-optic modulator (EOM), the pulse stream was split using a 3dB coupler and reflected off of two SSFBG encoders  $Q_1$ ,  $Q_2$  to generate 2 separate coded channels. The encoded signals were then fed onto SSFBG decoder  $Q_1^*$ . For the target user  $Q_1$ , the decoder generate a distinct auto-correlation peak with low level wings, while for improper user  $Q_2$ , the output will be low peak-level mutual cross-correlation function, namely, multiple access interference (MAI) noise. The decoded signal will be detected by the square law photo-detector (PD), where the mixing of the signal and interferences will result in the arising of beat noise. The receiver noise such as thermal and shot noise will arise in the receiver as well. Therefore, applying optical thresholding technique in the system to eliminate the interference noise is necessary. The optical thresholder (OT) could be inserted after the decoder to perform this function. In addition, optical thresholder could suppress auto-correlation wings to perform pulse shaping function for recoding.

To quantitatively evaluate the coding performance for coherent phase-coding OCDM system, two parameters are introduced in this paper: one is the ratio of

auto-correlation intensity peak over the maximum cross-correlation level (P/C ratio) for measuring the cross-correlation property, and another is the ratio of auto-correlation intensity peak over the maximum wing level (P/W ratio) as the measurement of the auto-correlation property.

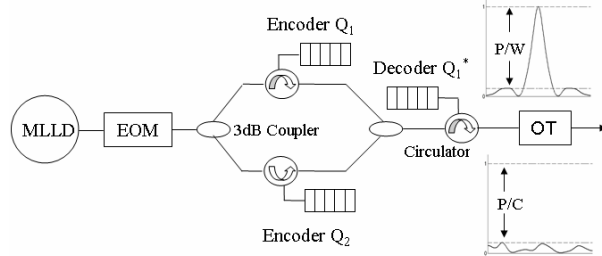


Fig. 1. System model of SSFBG-based OCDM system. MLLD: modelocked laser diode, EOM: electro-optic modulator, OT: optical thresholder.

### 3. NOLM based optical thresholder and NALM based optical thresholder

The optical thresholder based on nonlinear optical loop mirror (NOLM) is shown schematically in Fig. 2 (a), it consists of a loop of high nonlinear fiber (HNLF) formed between the output ports of a fiber coupler, and a polarization controller (PC) is employed. For the ultra-fast operation, a short length (135m) of HNLF is used. When a pulse is applied to an input terminal the coupler produces two components which traverse the common optical path, in opposite directions. They arrive back at the coupler simultaneously where they interfere, producing two outputs whose relative magnitudes depend on the phase between the two fields. High input pulse peak power and coupler with ratio  $\neq 0.5$  are required for the NOLM to suppress interference noise effectively.

Fig. 2 (b) depicts the configuration of the nonlinear amplifying loop mirror (NALM) based optical thresholder, the NALM itself consists of an bi-directional amplifier placed at one end of a 135 m long length of HNLF and joined in a loop by a 50:50 fiber coupler.

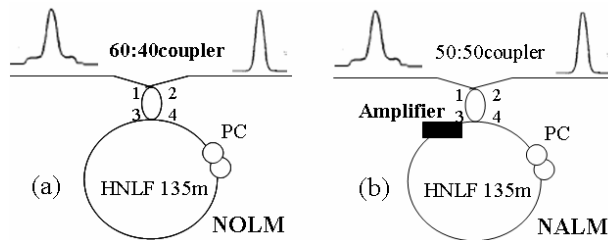


Fig. 2. Schematic diagram of NOLM based optical thresholder (a), and NALM based optical thresholder (b). HNLF: high nonlinear fiber; PC: polarization controller.

We assumed that the encoder and decoder to be

perfectly matched, pulse propagation within the NOLM and NALM was modeled using the nonlinear Schrödinger equation with group velocity dispersion and self-phase modulation as described by [7]

$$\frac{\partial U}{\partial z} + \frac{\alpha}{2}U + i\frac{\beta_2}{2}\frac{\partial^2 U}{\partial T^2} - \frac{\beta_3}{6}\frac{\partial^3 U}{\partial T^3} = i\gamma|U|^2U \quad (1)$$

where pulse amplitude  $U$  is normalized such that represents  $|U|^2$  the optical field strength within the fiber.  $\alpha$  represents the absorption coefficient and  $\gamma$  is the nonlinearity coefficient of the fiber. First order group velocity dispersion (GVD) $\beta_2$  and second order GVD $\beta_3$  relates to dispersion parameter  $D$  and dispersion slope  $dD/d\lambda$ , respectively. The values of these parameters of the HNLF at the system-operating wavelength of 1554nm were presented in Table 1 and corresponded to those of a fiber that was available within our laboratory.

Table 1. Parameters of the HNLF (at 1554 nm).

|                                                         |       |
|---------------------------------------------------------|-------|
| Length (m)                                              | 135   |
| Attenuation $\alpha$ (dB/km)                            | 0.51  |
| Nonlinear coefficient $\gamma$ (/W/km)                  | 20    |
| Dispersion $D$ (pm/nm/km)                               | 0.08  |
| Dispersion slope $dD/d\lambda$ (pm/nm <sup>2</sup> /km) | 0.034 |

### 4. Results and discussion

The encoder  $Q_1$ ,  $Q_2$  and decoder  $Q_1^*$  (see Fig.1) used within our following theoretical and experimental investigation are 4-phase shift superstructure fiber Bragg gratings (SSFBGs) [8]. The codes used are members of the Family A sequences. Compared to bipolar and unipolar coding, quaternary coding is known to provide codes with more desirable cross-correlation characteristics [9]. Each grating containing 7-chip has a uniform amplitude refractive index level along its length but in which discrete jumps in phase ( $0$ ,  $\pi/2$ ,  $\pi$ , or  $3\pi/2$ ) are written into the grating at the boundaries of adjacent spatial chips. The total length of the grating is 2.59 mm, and the individual chip length is 0.37 mm. This corresponds to a total code and chip duration of 25.1 and 3.6ps, respectively. The gratings are weakly reflecting SSFBGs (reflectivity typically  $< 20\%$ ). The SSFBG based approach relies upon the fact that the impulse response function of a weakly reflecting SSFBG follows directly the profile of the refractive-index superstructure function used to write the grating.

In the SSFBG-based OCDM system, the decoded pulse was amplified to a high power and then passed the

amplified pulses through the NOLM or NALM based optical threshold in order to selectively pass the correlation spike and filter out the low-level pedestal prior to detection. This nonlinear processing serves to further improve the signal-to-noise ratio (SNR) of the pattern-recognition signature and to reshape the correlation spike.

The transmissivity of the NALM as a function of input peak power is shown in Fig.3. As we can see, the optimum input peak power for the NALM is ~4 mW. In the calculation, saturate average power and small signal gain of the bi-directional amplifier is assumed to be 15 mW and 25 dB, respectively. In the calculation, the equation (1) was solved by using symmetrical split-step Fourier method.

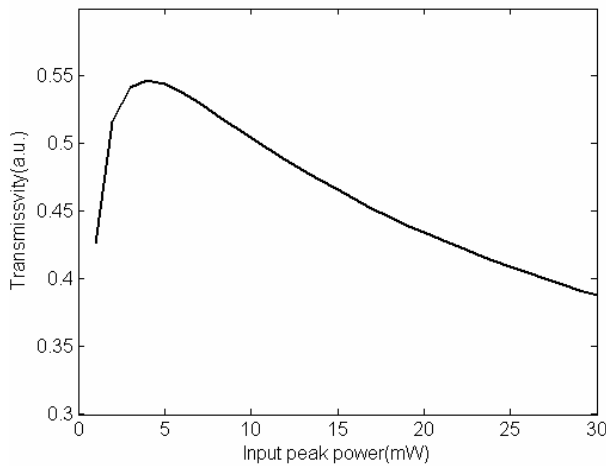


Fig.3. Transmissivity of the NALM as a function of input peak power.

To evaluate the impact of NOLM based optical thresholder on interference and pedestal rejection as a function of input pulse peak power, we plot P/W and P/C ratios of the decoded signals after the NOLM with three different couplers in Fig. 4. After simple en/decoding alone, the P/W and P/C ratio is 10.5 dB and 9.3 dB, respectively. However, at an input peak power of 5.0 W for the NOLM with 60:40 coupler, the ratios could be increased to 23.1 dB and 21.1 dB, respectively. As can be seen from Fig.2, the NOLM with 60:40 coupler could suppress interference and pedestal more effectively than 70:30 coupler and 80:20 coupler. The effect of NALM based optical thresholder on P/W and P/C ratios of the decoded signals is also shown in Fig.2(a) and Fig.2(b), respectively. With the optimum input peak power of 4 mW for NALM, the ratios could be increased to 29.8 dB and 26.1 dB, respectively. It is also found that the NALM could suppress interference and noise more effectively than the NOLM.

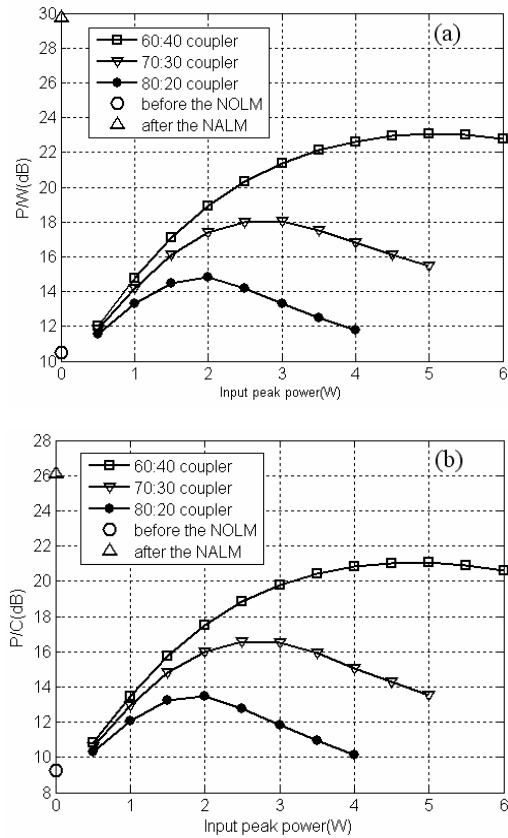


Fig.4. Impact of NOLM and NALM on the interference and pedestal rejection of decoded signal. (a) P/W ratio, (b) P/C ratio.  $\circ$ : after en/decoding alone,  $\Delta$ : after the NALM.

The experimental setup of OCDM system is similar as Fig. 1. The output pulse of the decoder  $Q_1^*$  could either be detected and characterized directly using a fast PD/Scope (~65GHz bandwidth) or pass through a optical thresholder (NOLM or NALM) before characterization. For NALM based optical thresholder, the input peak power is estimated to be ~ 5 mW. For NOLM based optical thresholder, the decoded pulse was amplified to an average power of ~0.5W corresponding to input peak power 3 W. The NOLM could also serve to improve the quality of the output signal, although the optimum input peak power 5W is not obtained due to the limitation of experimental condition. High power C-Band pre-amplified booster EDFA and Tektronix CSA8000B with optical module are employed. Several general EDFAs were included at various points in the system to restore the signal power.

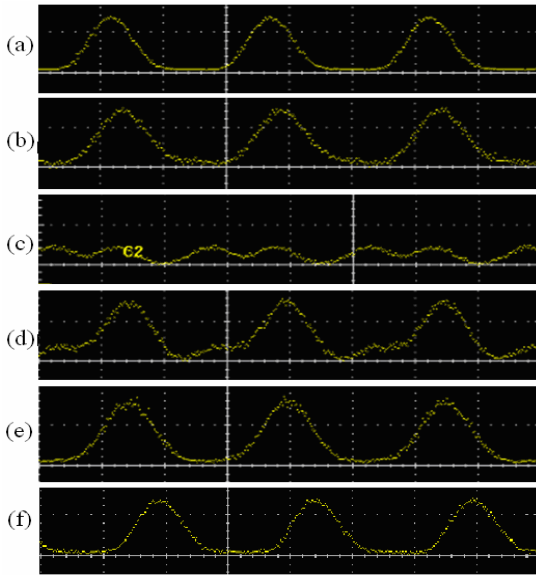


Fig.5. Oscilloscope traces of (a) incoming 1.3ps pulse stream, (b) decoded pulses (matched case:  $Q_1:Q_1^*$ ), (c) decode pulses (unmatched case:  $Q_2:Q_1^*$ ), (d) decode pulses ( $Q_1+Q_2:Q_1^*$ ), (e) decode pulses ( $Q_1+Q_2:Q_1^*$ ) after the NOLM, and (f) decode pulses ( $Q_1+Q_2:Q_1^*$ ) after the NALM. (Detection bandwidth:  $\sim 65\text{GHz}$ , vertical coordinates:  $2\text{mw/div}$ ; horizontal coordinates:  $10\text{ps/div}$ .)

We performed encoding-decoding experiments at 40 Gbit/s. Fig. 5 (a), (b) and (d) shows the degradation to the decoded signal traces as the number of OCDM channels is added into system compared with the original pulse trace. The pulse measurements were obtained using a fast photodiode and a sampling oscilloscope. Fig. 5 (c) shows trace for the decoded pulse under unmatched case  $Q_2:Q_1^*$ , short pulses are not reformed. As can be seen comparing the traces in Fig.5(b) and Fig.5(d), the effect of inter-channel interference noise is evident. The interference noise is due primarily to the temporal overlaps of two pseudo-orthogonal codes. The corresponding oscilloscope trace for the decoded pulse after the NOLM and NALM under 2-channel operation is presented in Fig. 5 (e) and Fig. 5 (f), respectively, which clearly show that short, distinct pulses are reformed. Fig.5(e) and Fig. 5 (f) confirm that interference and pedestal could be restrained apparently by using NOLM or NALM. For a more quantitative comparison, the measured extinction ratio (EXT) of the signal correspond to each trace in Fig.5 was presented in Table 2.

Table 2. Measured extinction ratio (EXT) of the signal correspond to each trace in Fig. 5.

| Output  | a    | b    | d   | e    | f    |
|---------|------|------|-----|------|------|
| EXT(dB) | 17.8 | 10.1 | 6.5 | 12.6 | 16.2 |

The results of Figs. 4 and 5 and Table 2 validate that both NOLM and NALM could act as a nonlinear processing element capable to reduce interference and noise in the OCDM system effectively.

## 5. Conclusions

NOLM and NALM based optical thresholding techniques in OCDM system are analyzed. The theoretical results build the effectiveness of NOLM and NALM based on HNLFF for interference and noise rejecting. For the NOLM based optical thresholder, with optimum input peak power of 5 W and 60:40 coupler, the P/W and P/C ratio could be increased to 23.1 dB and 21.1 dB, respectively. While for the NALM based optical thresholder, with optimum input peak power of 4 mW, the P/W and P/C ratio could be increased to 29.8 dB and 26.1 dB, respectively. Moreover, the system benefits of using NOLM and NALM are also experimental demonstrated.

## Acknowledgments

This work was supported by the National Science Foundation of China under Grant 60577007.

## References

- [1] K. Kitayama, IEEE J. Select. Areas Commun. **16**(9), 1309 (1998).
- [2] P. C. Teh, P. Petropoulos, M. Ibsen, D. J. Richardson, IEEE Photon Technol.Lett. **13**(2), 154, (2001).
- [3] N. J. Doran, D. Wood, Opt. Lett. **13**(1), 56 (1988).
- [4] N. J. Smith, N. J. Doran, J. Opt. Soc. Am. B **12**(6), 1117 (1995).
- [5] A. W. Oneill, R. P. Webb, Electron.Lett. **26**(24), 2008 (1990).
- [6] E. Yamada, M. Nakazawa, IEEE Journal of Quantum Electronics **30**(8), 1842 (1994).
- [7] G. P. Agrawal, Nonlinear Fiber Optics [M]. New York: Academic 43, 1995.
- [8] Xiaogang Chen, Dexiu Huang, Xiuhua Yuan, Optical Engineering **46**(1), 015006 (2007).
- [9] S. Boztas, R. Hammons, P. V. Kumar, IEEE Trans. Information Theory **38**(3), 1101 (1992).

\*Corresponding author: cxg826@yahoo.com.cn